*Journal of Sound and Vibration* (2002) **249**(1), 83–100
doi:10.1006/jsvi.2001.3854, available online at http://www.idealibrary.com on IDEAL®

# A STOCHASTIC NEWMARK METHOD FOR ENGINEERING DYNAMICAL SYSTEMS

D. Roy and M. K. Dash

*Department of Civil Engineering, Indian Institute of Technology, Kharagpur* 721 302, *India.*
*E-mail*: *royd@civil.iitkgp.ernet.in*

(*Received* 4 *October* 2000, *and in final form* 1 *June* 2001)

The purpose of this study is to develop a stochastic Newmark integration principle based on an implicit stochastic Taylor (Ito–Taylor or Stratonovich–Taylor) expansion of the vector field. As in the deterministic case, implicitness in stochastic Taylor expansions for the displacement and velocity vectors is achieved by introducing a couple of non-unique integration parameters, $\alpha$ and $\beta$. A rigorous error analysis is performed to put bounds on the local and global errors in computing displacements and velocities. The stochastic Newmark method is elegantly adaptable for obtaining strong sample-path solutions of linear and non-linear multi-degree-of freedom (m.d.o.f.) stochastic engineering systems with continuous and Lipschitz-bounded vector fields under (filtered) white-noise inputs. The method has presently been numerically illustrated, to a limited extent, for sample-path integration of a hardening Duffing oscillator under additive and multiplicative white-noise excitations. The results are indicative of consistency, convergence and stochastic numerical stability of the stochastic Newmark method (SNM).



## 1. INTRODUCTION

Newmark method is by far the most popular tool for direct integration of deterministic dynamical systems [1–4]. For a given time step size, $h$, a Newmark map may be derived by expanding the displacement and velocity components upto $O(h^2)$ and $O(h)$, respectively, via a two-parameter implicit Taylor series. This corresponds to a constant average acceleration for a sufficiently continuous deterministic system. The same logic, however, cannot be directly used for stochastic systems under white-noise inputs. It is well known that a white-noise process, defined as the derivative of a Wiener process, is not a valid mathematical function of time. This is because a Wiener process, even though continuous, may have an unbounded variation over any given time interval. Consequently, for such engineering systems, the acceleration vector does not exist mathematically (at least, in the sense of sample paths). Moreover, increments of a Wiener process change by $O(h^{1/2})$ over a time interval of $h$. These two non-deterministic aspects of a stochastic differential equation (SDE) explain why numerical integration techniques for strong solutions of SDEs are often so different from their deterministic counterparts [5]. A consistent way to achieve higher order accuracy while developing numerical algorithms for pathwise (strong) solutions of SDEs is to use a stochastic Taylor expansion [6]. The stochastic Euler method, which constitutes a stochastic Taylor expansion by retaining terms upto $O(h)$ (but not including all of them), has $O(h)$ and $O(h^{1/2})$ local and global errors of convergence respectively [7–9]. Milstein [10] has also proposed a strong Taylor scheme of local error $O(h)$. Strong Taylor schemes of $O(h^{3/2})$ and $O(h^2)$ have been proposed, among others, by Wagner and Platen [11], Milstein [12] and Kloeden and Platen [13] by adding more terms to the Milstein scheme. An extensive review of all these methods are found in reference [6]. A difficulty in using these higher order Taylor approximations is the evaluation of first and higher order derivatives of the drift and diffusion terms. This is compounded with the daunting task of numerically evaluating the multiple Ito (or, Stratonovich) integrals. As an alternative, Rumelin [14] has systematically investigated stochastic Runge–Kutta schemes of strong order 1·0. For SDEs driven by a one-dimensional Wiener process, a second order stochastic Runge–Kutta scheme, known as the stochastic Heun scheme (SHS), is, by far, the most general as well as an accurate integration scheme of strong (local) order 1·5 [5]. *However, for SDEs with a higher-dimensional Wiener vector, SHS only yields a local error of order* 1·0 *unless certain conditions on the gradients of the diffusion terms are met with.* In fact, Rumelin [14] has proved that Runge–Kutta methods can have an accuracy of higher order than the SHS if and only if certain very restrictive equalities involving the partial derivatives of the drift and diffusion coefficients are satisfied.

It may be relevant to mention the work of To [15–18] and Zhang and Zhao [19], Zhang *et al.* [20] on the developments of finite difference techniques and the Newmark method for direct integration of SDEs of engineering interest. Using the auto-regressive model, Miao [21] has developed a central difference algorithm for dynamical systems under non-stationary excitations. These studies are possibly applicable to systems driven by non-white random excitations with bounded variations. None of these studies, however, adequately account for the typical sample-path characteristics of Wiener increments when the random inputs are modelled as (filtered) white-noise processes.

To start developing a stochastic Newmark method (SNM), a few continuity and boundedness requirements on the drift and diffusion vectors are first imposed. The stochastic Newmark map is then derived by appropriate stochastic Taylor expansions of the displacement and velocity vectors in terms of a given time step size, $h$. Following the deterministic Newmark principle, displacement and velocity expansions are performed implicitly using a couple of integration parameters, $\alpha$ and $\beta$. As in the deterministic case, the displacement and velocity expansions are, respectively, obtained by retaining terms upto $O(h^2)$ and $O(h)$ for a given a time step size $h$. Interestingly, certain terms of the highest order in $h$, i.e., terms of $O(h^2)$ or $O(h)$ as the case may be, involving multiple stochastic integrals in terms of the Wiener increments, are dropped from these expansions for computational expedience. A rigorous error estimate is then carried out to determine the local and global error orders for both displacement and velocity vectors. A limited numerical implementation of the method is presently undertaken for a non-linear hardening Duffing oscillator under additive and multiplicative white noise inputs.

## 2. METHOD OF ANALYSIS

Since the stochastic Newmark method (SNM) is expected to be used mostly in engineering dynamics, a natural starting point would be to consider the following $n$-d.o.f. dynamical system:

$$\ddot{X} + C(X, \dot{X})\dot{X} + K(X, \dot{X})X = \sum_{r=1}^{q} G_r(X, \dot{X}, t)\,\dot{W}_r + B(t), \tag{1}$$

where $X = \{x^{(1)}\,\dot{x}^{(1)}\,x^{(2)}\,\dot{x}^{(2)}\ldots x^{(n)}\,\dot{x}^{(n)}\}^{\mathrm{T}} \in \mathbb{R}^{2n}$, $C(X, \dot{X})$, $K(X, \dot{X})$ are $n \times n$ (state dependent for non-linear systems) damping and stiffness matrices, $\{G_r(X, \dot{X}, t)\}$ is the $r$th element of a set of $n \times 1$ diffusion vectors, $\{W_r(t)\}$ constitutes a $q$-dimensional vector of independently evolving zero mean Wiener processes with $W_r(t)$, $r = 1, 2, \ldots, q$ with $W_r(0) = 0$, $E[|W_r(t) - W_r(s)|^2] = (t - s), t > s$ and $B(t) = \{b^{(j)}(t) | j = 1, 2, \ldots, n\}$ is the external (non-parametric) deterministic force vector. The description of the dynamical system as in equation (1) being entirely formal, they may more appropriately be recast as the following system of $2n$ first order equations in an incremental form in the state space:

$$\mathrm{d}x_1^{(j)} = x_2^{(j)},$$

$$\mathrm{d}x_2^{(j)} = a^{(j)}(X, \dot{X}, t) + \sum_{r=1}^{q} \sigma_r^{(j)}(X, \dot{X}, t)\, \mathrm{d}W_r(t), \quad j = 1, 2, \ldots, n, \tag{2}$$

where

$$a^{(j)}(X, \dot{X}, t) = -\sum_{k=1}^{n} C_{jk}(X, \dot{X}) \dot{x}^{(k)} - \sum_{k=1}^{n} K_{jk}(X, \dot{X}) x^{(k)} + b^{(j)}(t),$$

$$\sigma_r^{(j)}(X, \dot{X}, t) = G_r^{(j)}(X, \dot{X}, t). \tag{3}$$

In order to ensure sample existence and boundedness of the solution vectors $X = \{x_1^{(j)}\}$ and $\dot{X} = \{x_2^{(j)}\}$, $j = 1, 2, \ldots, n$, it is assumed that the drift and diffusion vectors, $a^{(j)}$ and $\sigma_r^{(j)}$ are measurable (with respect to $t \in \mathbb{R}^1$, $X, \dot{X} \in \mathbb{R}^n$), continuous and satisfy the Lipschitz growth bound:

$$|a^{(j)}(\bar{X}, t) - a^{(j)}(\bar{Y}, t)| + \sum_{r=1}^{q} |\sigma_r^{(j)}(\bar{X}, t) - \sigma_r^{(j)}(\bar{Y}, t)| \leqslant Q \|\bar{X} - \bar{Y}\|, \quad \forall j \in [1, n], \tag{4}$$

where $\bar{X}, \bar{Y} \in \mathbb{R}^{2n}$ and $\bar{X} = \{X\ \dot{X}\}^{\mathrm{T}} = \{X_1\ X_2\}^{\mathrm{T}}$. The norm $\|\cdot\|$ is the Euclidean norm. Let the initial conditions be mean square bounded, i.e., $\mathbf{E}\|\bar{X}(t_0)\|^2 < \infty$. and have certain growth bounds (not necessarily linear). Thus, the sample continuity (w.p.1) of any realization of the (separable) vector flow $\phi(t, \omega, \bar{X}(t_0))$ for any $\omega \in \Omega$ ($\Omega$ being the event space) is assured. Let the subset of the time axis over $[0, \tau]$ be ordered such that $0 = t_0 < t_1 < t_2 < \cdots < t_i < \cdots < t_L = \tau$ and $h_i = t_i - t_{i-1}$ where $i \in Z^+$. It is now required to replace the non-linear system of SDEs (1) by a suitably determined (stochastic) Newmark map over the $i$th time interval $T_i = (t_{i-1}, t_i]$, given the initial condition vector $\bar{X}(t_{i-1}) \triangleq \bar{X}_{i-1}$. It is assumed that the response random variable $\bar{X}(t_i) \triangleq \bar{X}_i$ is $\mathscr{F}(t_i)$ measurable with $\mathbf{E}\|\bar{X}_i\|^2 < \infty$ and $\mathscr{F}(t_i)$ denoting the non-increasing family of $\sigma$-subalgebras. Further, for convenience of discussion, a uniform time step size $h_i = h\ \forall i$ is assumed.

Now, towards deriving the stochastic Newmark map over the $i$th time interval, the first step is to consider equation (2) and expand each element of the vectors $X_1(t_{i-1} + h) = X(t_{i-1} + h)$ and $X_2(t_{i-1} + h) = \dot{X}_1(t_{i-1} + h)$ in a stochastic Taylor expansion around $X_1(t_{i-1}) = X_{1,i-1}$ and $X_2(t_{i-1}) = X_{2,i-1}$ respectively. In the present study, the derivation of the map is performed following Ito's formula, which, as adapted specifically for equation (2), is stated below:

$$f(X_1(s), X_2(s), s) = f(X_1(t_{i-1}), X_2(t_{i-1}), t_{i-1}) + \sum_{r=1}^{q} \int_{t_{i-1}}^{s} \Lambda_r f(X_1(s_1), X_2(s_1), s_1)\, \mathrm{d}W_r(s_1)$$

$$+ \int_{t_{i-1}}^{s} Lf(X_1(s_1), X_2(s_1), s_1)\, \mathrm{d}s_1, \tag{5a}$$

where $f$ is any sufficiently smooth (scalar or vector) function of its arguments, $s \geqslant t_{i-1}$ and the operators $\Lambda_r$ and $L$ are given by

$$\Lambda_r = \sum_{j=1}^{n} \sigma_r^{(j)} \frac{\partial f(X_1, X_2, t)}{\partial x_2^{(j)}}, \tag{5b}$$

$$L = \frac{\partial f}{\partial t} + \sum_{j=1}^{n} x_2^{(j)} \frac{\partial f}{\partial x_1^{(j)}} + \sum_{j=1}^{n} a^{(j)} \frac{\partial f}{\partial x_2^{(j)}} + 0{\cdot}5 \sum_{r=1}^{q} \sum_{k=1}^{n} \sum_{l=1}^{n} \sigma_r^{(k)} \sigma_r^{(l)} \frac{\partial^2 f}{\partial x_2^{(k)} \partial x_2^{(l)}}. \tag{5c}$$

Now the $j$th element, $x_1^{(j)}(t_{i-1}+h)$, of the $n$-dimensional vector $X_1(t_{i-1}+h)$ is expanded in a stochastic Taylor expansion as

$$\begin{aligned} x_1^{(j)}(t_{i-1}+h) &= x_1^{(j)}(t_{i-1}) + \int_{t_{i-1}}^{t_i} x_2^{(j)}(s)\,\mathrm{d}s \\ &= x_1^{(j)}(t_{i-1}) + \int_{t_{i-1}}^{t_i} \{x_2^{(j)}(t_{i-1}) + \int_{t_{i-1}}^{s} a^{(j)}(\bar{X}(s_1), s_1)\,\mathrm{d}s_1 \\ &\quad + \sum_{r=1}^{q} \int_{t_{i-1}}^{s} \sigma_r^{(j)}(\bar{X}(s_1), s_1)\,\mathrm{d}W_r(s_1)\}\,\mathrm{d}s. \end{aligned} \tag{6}$$

At this stage, Ito's formula may be applied on the functions $\sigma_r^{(j)}$ and $a^{(j)}$ around $(\bar{X}(t_{i-1}), t_{i-1})$ to obtain

$$\begin{aligned} x_1^{(j)}(t_i) &= x_1^{(j)}(t_{i-1}) + x_2^{(j)}(t_{i-1})h + a^{(j)}(\bar{X}(t_{i-1}), t_{i-1})\frac{h^2}{2} \\ &\quad + \sum_{r=1}^{q} \sigma_r^{(j)}(\bar{X}(t_{i-1}), t_{i-1}) \int_{t_{i-1}}^{t_i} \int_{t_{i-1}}^{s} \mathrm{d}W_r(s_1)\,\mathrm{d}s + \rho_1^{(j)}, \end{aligned} \tag{7a}$$

where the $j$th remainder component, $\rho_1^{(j)}$, consists of the following multiple integrals:

$$\begin{aligned} \rho_1^{(j)} &= \sum_{r=1}^{q} \int_{t_{i-1}}^{t_i} \int_{t_{i-1}}^{s} \int_{t_{i-1}}^{s_1} \Lambda_r a^{(j)}(\bar{X}(s_2), s_2)\,\mathrm{d}W_r(s_2)\,\mathrm{d}s_1 \mathrm{d}s \\ &\quad + \int_{t_{i-1}}^{t_i} \int_{t_{i-1}}^{s} \int_{t_{i-1}}^{s_1} L a^{(j)}(\bar{X}(s_2), s_2)\,\mathrm{d}s_2\,\mathrm{d}s_1\,\mathrm{d}s \\ &\quad + \sum_{r=1}^{q} \sum_{l=1}^{q} \int_{t_{i-1}}^{t_i} \int_{t_{i-1}}^{s} \int_{t_{i-1}}^{s_1} \Lambda_l \sigma_r^{(j)}(\bar{X}(s_2), s_2)\,\mathrm{d}W_l(s_2)\,\mathrm{d}W_r(s_1)\,\mathrm{d}s \\ &\quad + \sum_{r=1}^{q} \int_{t_{i-1}}^{t_i} \int_{t_{i-1}}^{s} \int_{t_{i-1}}^{s_1} L\sigma_r^{(j)}(\bar{X}(s_2), s_2)\,\mathrm{d}s_2\,\mathrm{d}W_r(s_1)\,\mathrm{d}s. \end{aligned} \tag{7b}$$

The above equations constitute a direct stochastic Taylor expansion for the displacement vector $X_1$. However, keeping in mind the deterministic Newmark technique, an implicitness is introduced in the expansion by using a non-unique real integration parameter $\alpha$ and writing equation (7a) as

$$x_1^{(j)}(t_i) = x_1^{(j)}(t_{i-1}) + x_2^{(j)}(t_{i-1})h + \sum_{r=1}^{q} \sigma_r^{(j)}(\bar{X}(t_{i-1}), t_{i-1}) \int_{t_{i-1}}^{t_i} \int_{t_{i-1}}^{s} \mathrm{d}W_r(s_1)\,\mathrm{d}s$$

$$+ \alpha\, a^{(j)}(\bar{X}(t_{i-1}), t_{i-1}) \frac{h^2}{2} + (1-\alpha)\, a^{(j)}(\bar{X}(t_{i-1}), t_{i-1}) \frac{h^2}{2} + \rho_1^{(j)}. \tag{8}$$

Now the fifth term on the right-hand side of the above equation is expressed in terms of $a^{(j)}(\bar{X}(t_i), t_i)$ via a backward stochastic Taylor expansion as

$$a^{(j)}(\bar{X}(t_{i-1}), t_{i-1}) = a^{(j)}(\bar{X}(t_i), t_i) - \rho_2^{(j)}, \tag{9a}$$

where the remainder $\rho_2^{(j)}$ is given by

$$\rho_2^{(j)} = \int_{t_{i-1}}^{t_i} L a^{(j)}(\bar{X}(s), s)\,\mathrm{d}s + \sum_{r=1}^{q} \int_{t_{i-1}}^{t_i} \Lambda_r a^{(j)}(\bar{X}(s), s)\,\mathrm{d}W_r(s). \tag{9b}$$

Thus, one has the following expression for $x_1^{(j)}(t_i) \triangleq x_{1,i}^{(j)}$:

$$x_{1,i}^{(j)} = x_{1,i-1}^{(j)} + x_{2,i-1}^{(j)}\, h + \sum_{r=1}^{q} \sigma_r^{(j)}(\bar{X}_{i-1}, t_{i-1}) \int_{t_{i-1}}^{t_i} \int_{t_{i-1}}^{s} \mathrm{d}W_r(s_1)\,\mathrm{d}s + \alpha\, a^{(j)}(\bar{X}_{i-1}, t_{i-1}) \frac{h^2}{2}$$

$$+ (1-\alpha)\, a^{(j)}(\bar{X}_i, t_i) \frac{h^2}{2} + R^{(j)}, \tag{10a}$$

$$R^{(j)} = -(1-\alpha)\,\rho_2^{(j)} \frac{h^2}{2} + \rho_1^{(j)}. \tag{10b}$$

The $j$th velocity component $x_{2,i}^{(j)}$ is now implicitly expanded as

$$x_{2,i}^{(j)} = x_{2,i-1}^{(j)} + \sum_{r=1}^{q} \sigma_r^{(j)}(\bar{X}_{i-1}, t_{i-1}) \int_{t_{i-1}}^{t_i} \mathrm{d}W_r(s) + \beta a^{(j)}(\bar{X}_{i-1}, t_{i-1})h$$

$$+ (1-\beta)\, a^{(j)}(\bar{X}_i, t_i)\, h + R_1^{(j)}, \tag{11}$$

where the expression for the remainder is

$$R_1^{(j)} = \sum_{r=1}^{q} \int_{t_{i-1}}^{t_i} \mathrm{d}W_r(s) \int_{t_{i-1}}^{s} \sum_{l=1}^{q} \Lambda_l \sigma_r^{(j)}(\bar{X}(s_1), s_1)\,\mathrm{d}W_l(s_1)$$

$$+ \sum_{r=1}^{q} \int_{t_{i-1}}^{t_i} \mathrm{d}W_r(s) \int_{t_{i-1}}^{s} L\sigma_r^{(j)}(\bar{X}(s_1), s_1)\,\mathrm{d}s_1 - (1-\beta)\,\rho_2^{(j)}\, h. \tag{12}$$

In the right-hand side of the above expression, $\rho_2^{(j)}$ is given by equation (9b). Now a stochastic Newmark map for the $j$th scalar displacement, $x_1^{(j)}$, is given by equation (10a) without the last remainder term, $R^{(j)}$, on the right-hand side. Similarly, a Newmark map for the $j$th scalar velocity, $x_2^{(j)}$, is obtained via equation (11) without the remainder term $R_1^{(j)}$ on the right-hand side. These Newmark approximations to $\{\bar{X}\} = \{\{x_1^{(j)}\}\,\{x_2^{(j)}\}\,|\, j = 1, 2, \ldots, n\}$ will henceforth be denoted as $\{\tilde{X}\} = \{\{\tilde{x}_1^{(j)}\}\,\{\tilde{x}_2^{(j)}\}\,|\, j = 1, 2, \ldots, n\}$.

## 3. ERROR ESTIMATES

Since the sample path, $\bar{X}(t)$ traced by the given SDE is, in general, different from the approximated Newmark solution, $\tilde{X}$, an instantaneous error at $t = t_i$ may be defined as the $2n$-dimensional vector $E_i = \{E_{1,i}^{(j)}\, E_{2,i}^{(j)}\} = \{(x_{1,i}^{(j)} - \tilde{x}_{1,i}^{(j)}), (x_{2,i}^{(j)} - \tilde{x}_{2,i}^{(j)})\}$, where $j = 1, \ldots, n$, and the instantaneous Euclidean error norm is denoted as $e_i = \|\bar{X}_i - \tilde{X}_i\|$. This error vector is treated as a set of conditional random variables such that the local initial condition, $\bar{X}_{i-1}$, is deterministic and that $\bar{X}_{i-1} = \tilde{X}_{i-1}$. In what follows, let $c_m$ and $c_s$, respectively, denote the orders of the mean and mean square of this conditional (local) error with respect to the chosen time step size, $h = t_i - t_{i-1}$. In other words, one has the following bounds:

$$\|\mathbf{E}(\bar{X}_i - \tilde{X}_i)\| \leqslant Q(1 + \|\bar{X}_{i-1}\|^2)\, h^{c_m}, \tag{13}$$

$$[\mathbf{E}\,\|\bar{X}_i - \tilde{X}_i\|^2]^{1/2} \leqslant Q(1 + \|\bar{X}_{i-1}\|^2)\, h^{c_s}. \tag{14}$$

Also, let $c_s \geqslant 1/2$ and $c_m \geqslant c_s + 1/2$. Then, one has the following bound on the global error:

$$[\mathbf{E}\,\|\bar{X}_i - \tilde{X}_i\|^2]^{1/2} \leqslant Q(1 + \|\bar{X}_0\|^2)\, h^{c_s - 1/2}. \tag{15}$$

This implies that the global order of accuracy of the method, constructed using a one-step approximation, is $c_g = c_s - 1/2$. Milstein [12] has provided a detailed proof of this observation. From the remainder equations 7(b), 9(b) and (12), it is clear that for evaluating the mean and mean-square error orders, it is necessary to determine the first two statistical moments of certain multiple integrals, generally denoted by

$$I_{j_1,\, j_2, \ldots,\, j_k} = \int_{t_{i-1}}^{t_i} \mathrm{d}W_{j_k}(s) \int_{t_{i-1}}^{s} \mathrm{d}W_{j_{k-1}}(s_1) \int_{t_{i-1}}^{s_1} \cdots \int_{t_{i-1}}^{s_{k-2}} \mathrm{d}W_{j_1}(s_{k-1}), \tag{16}$$

where the integers $j_1, j_2, \ldots, j_k$ take values in the set $\{0, 1, 2, \ldots, q\}$ and $I_{j_1,\, j_2, \ldots,\, j_k}$ may be considered as the $k$th Ito multiple integral. Moreover, $\mathrm{d}W_0(s)$ is taken to indicate $\mathrm{d}s$. At this stage, the following proposition becomes quite relevant.

**Proposition 1.** *One has* $\mathbf{E}(I_{j_1,\, j_2, \ldots,\, j_k}) = 0$ *if there exists at least one* $j_l \neq 0$, $l = 1, 2, \ldots, k$. *On the other hand*, $\mathbf{E}(I_{j_1,\, j_2, \ldots,\, j_k}) = O(h^k)$ *if* $j_l = 0\ \forall\, l \in [0, k]$. *Moreover*,

$$[\mathbf{E}(I_{j_1,\, j_2, \ldots,\, j_k})^2]^{1/2} = O(h^w),$$

*where*

$$w = \sum_{l=1}^{k} (2 - \bar{j}_l)/2, \bar{j}_l = 1 \text{ if } j_l \neq 0, \quad \text{else} \quad \bar{j}_l = 0. \tag{17}$$

Proof of the first part of the above proposition regarding the mean is quite straightforward. For the second part, involving equation (17), reference is made to the monographs by Milstein [12] or Kloeden and Platen [6].
Now taking expectation of the remainder term $R^{(j)}$ associated with the $j$th displacement component $x_{1,i}^{(j)}$ (equations 10(a) and 10(b)), one can readily see via Proposition 1 and inequality (13) that

$$|\mathbf{E}R^{(j)}| \leqslant Q(1 + \|\bar{X}_{i-1}\|^2)\,h^3. \tag{18a}$$

Similarly, using equation (17) and inequality (14), it follows that

$$|\mathbf{E}(R^{(j)})^2|^{1/2} \leqslant Q(1 + \|\bar{X}_{i-1}\|^2)^{1/2}\,h^2. \tag{18b}$$

Thus, for the proposed stochastic Newmark scheme as applied to displacements, one has $(c_m)_x = 3$, $(c_s)_x = 2\ (>\frac{1}{2})$, and thus the inequality $(c_m)_x \geqslant (c_s)_x + 1/2$ is satisfied. Hence, the global error order for computing the displacement vector is given by $(c_g)_x = 1{\cdot}5$. One can also apply the above arguments for the velocity equation (11) and the associated remainder equation (12) to obtain $(c_m)_{\dot{x}} = 2$, $(c_s)_{\dot{x}} = 1\ (>\frac{1}{2})$. Thus, the inequality $(c_m)_{\dot{x}} \geqslant (c_s)_{\dot{x}} + 1/2$ is again satisfied to yield $(c_g)_{\dot{x}} = \frac{1}{2}$.

It is of interest to note here that the implicit stochastic Taylor expansion of equation 10(a) used to obtain the Newmark approximation, $\tilde{x}_{1,i}^{(j)}$, to the exact displacement component, $x_{1,i}^{(j)}$, is not complete in $O(h^2)$. If, in addition, the other easily evaluatable $O(h^2)$ term, $u_1 = \alpha a^{(j)}(\bar{X}_{i-1}, t_{i-1})\,h^2/2 + (1-\alpha)\,a^{(j)}(\bar{X}_i, t_i)\,h^2/2$, is also left out of the expansion, then from Proposition 1 one would have $(c_m)_x = 2$, $(c_s)_x = 2$. Since the inequality $(c_m)_x \geqslant (c_s)_x + 0{\cdot}5$ is no longer satisfied, one must take $(c_s)_x = 1{\cdot}5$ for evaluating the global error order $(c_g)_x$ [6]. Thus, one finally has $(c_g)_x = 1{\cdot}5 - 0{\cdot}5 = 1{\cdot}0$. Hence, it is observed that even though the presently adopted Newmark expansion is not complete in $O(h^2)$, retaining the term $u_1$ leads to an increase in $(c_g)_x$ by 0·5. Now, consider the other possibility of retaining the term involving the $O(h^2)$ integral $I_{l,r,0}$ in the expansion instead of the term $u_1$. In such a case, one readily obtains, again via Proposition 1, $(c_m)_x = 2$, $(c_s)_x = 2$. Thus, one again gets $(c_g)_x = 1{\cdot}0$, i.e., 0·5 less in order than is achieved by retaining $u_1$ instead of the term involving $I_{l,r,0}$. However, if both these $O(h^2)$ terms are included, then $(c_m)_x = 3{\cdot}0$, $(c_s)_x = 2{\cdot}5$, and hence $(c_g)_x = 2{\cdot}0$, i.e., 0·5 more in order than the presently adopted scheme at the cost of an enhanced computational effort, which sharply increases with an increase in the system d.o.f. Similar arguments as above may be used to justify the inclusion of the $O(h)$ term, $u_2 = \beta a^{(j)}(\bar{X}_{i-1}, t_{i-1})h + \beta a^{(j)}(\bar{X}_i, t_i)h$, and not the term involving $O(h)$ multiple Ito integral $I_{l,r}$ $(l, r \neq 0)$. Finally, it may be noted that computations of error orders along with the retention of appropriate terms in SNM considerably differ from those for its well-known deterministic counterparts. Moreover, one can theoretically propose consistently higher order versions of SNM for achieving better accuracy levels.

## 4. ILLUSTRATIVE EXAMPLES

For an example problem, consider the non-linear second order SDE for the hardening Duffing oscillator under a deterministic sinusoidal excitation and a couple of additive and multiplicative white-noise excitations, adequately described by the following five-parameter equation [22]:

$$\ddot{x} + 2\pi\varepsilon_1\dot{x} + 4\pi^2\varepsilon_2(1 + x^2)x - \varepsilon_5 x\dot{W}_2 = 4\pi^2\varepsilon_3\cos(2\pi t) + \varepsilon_4\dot{W}_1(t). \tag{19}$$

Since differentiation of Wiener processes, i.e., $\dot{W}_1(t)$, $\dot{W}_2(t)$ cannot be mathematically accomplished in a pathwise sense, the SDE is more appropriately written in the following incremental state-space form:

$$\mathrm{d}x_1(t) = x_2(t)\,\mathrm{d}t \; \mathrm{d}x_2(t) = (-2\pi\varepsilon_1 x_2 - 4\pi^2\varepsilon_2(1 + x_1^2)x_1 + \varepsilon_5 x_1\,\mathrm{d}W_2(t) + 4\pi^2\varepsilon_3\cos(2\pi t))\,\mathrm{d}t + \varepsilon_4\,\mathrm{d}W_1(t). \tag{20}$$

Following equations (10) and (11) with $n = 1$, one obtains the following Newmark approximation $\tilde{X} = \{\tilde{x}_{1,i}, \tilde{x}_{2,i}\}$ for the desired solution $\bar{X} = \{x_{1,i}, x_{2,i}\}$:

$$\tilde{x}_{1,i} = x_{1,i-1} + x_{2,i-1}h + \varepsilon_4\int_{t_{i-1}}^{t_i}\int_{t_{i-1}}^{s}\mathrm{d}W_1(s_1)\,\mathrm{d}s + \varepsilon_5 x_{1,i-1}\int_{t_{i-1}}^{t_i}\int_{t_{i-1}}^{s}\mathrm{d}W_2(s_1)\,\mathrm{d}s + \alpha\, a(\bar{X}_{i-1}, t_{i-1})\frac{h^2}{2} + (1-\alpha)\,a(\bar{X}_i, t_i)\frac{h^2}{2}, \tag{21a}$$

$$\tilde{x}_{2,i} = x_{2,i-1} + \varepsilon_4\int_{t_{i-1}}^{t_i}\mathrm{d}W_1(s) + \varepsilon_5 x_{1,i-1}\int_{t_{i-1}}^{t_i}\mathrm{d}W_2(s) + \beta a(\bar{X}_{i-1}, t_{i-1})\,h + (1-\beta)\,a(\bar{X}_i, t_i)\,h, \tag{21b}$$

where $a(\bar{X}, t) = -2\pi\varepsilon_1 x_2 - 4\pi^2\varepsilon_2(x_1 + x_1^3) + 4\pi^2\varepsilon_3\cos(2\pi t)$.
Note that the superscript $^{(j)}$ has been omitted from the state variables since $n = 1$. For a computer implementation of SNM, it is first observed that the couple of stochastic integrals in equation 21(b) are given by

$$I_l = \int_{t_{i-1}}^{t_i}\mathrm{d}W_l(s) = W_l(t_i) - W_l(t_{i-1}) = W_{l,i} - W_{l,i-1} \triangleq \Delta W_{l,i}, \quad l = 1, 2. \tag{22}$$

These $i$th Wiener increments may straightaway be generated via the $i$th elements, $q_{l,i}$, of two independently generated semi-infinite sequences, $\Lambda_l = \{\varsigma_{l,i}\}$ $(l = 1, 2)$, of zero-mean and unit-variance Gaussian random variables and using the equation:

$$\Delta W_{l,i} = h^{1/2}\varsigma_{l,i}. \tag{23}$$

The well-known Box–Muller transformation may be used to obtain these standard Gaussian variables, $\varsigma_{l,i}$. It is now needed to numerically generate the double stochastic integrals, $I_{l,0}$ $(l = 1, 2)$, appearing in Newmark displacement map of equation 21(a). Towards this, the following estimates are first performed [12]:

$$\mathbf{E}\left[\Delta W_{l,i}\left\{\int_{t_{i-1}}^{t_i}(W_l(s) - W_{l,i-1})\,\mathrm{d}s - 0{\cdot}5h\Delta W_{l,i}\right\}\right] = 0, \quad \mathbf{E}(\Delta W_{l,i})^2 = h, \tag{24a, 24b}$$

$$\mathbf{E}\left\{\int_{t_{i-1}}^{t_i}(W_l(s) - W_{l,i-1})\,\mathrm{d}s - 0{\cdot}5h\Delta W_{l,i}\right\}^2 = h^3/12. \tag{24c}$$

The new random variables, $\int_{t_{i-1}}^{t_i}(W_l(s) - W_{l,i-1})\,\mathrm{d}s - 0{\cdot}5h\Delta W_{l,i}$, are zero-mean Gaussian variables with a standard deviation of $h^{3/2}/\sqrt{12}$ and are uncorrelated with Wiener increments $\Delta W_{l,i}$. These new random variables may be obtained by generating another couple of semi-infinite sequences, $\Gamma_l = \{\zeta_{l,i}\}$, of standard (zero-mean, unit-variance) Gaussian random variables followed by using the equation:

$$\int_{t_{i-1}}^{t_i} (W_l(s) - W_{l,i-1})\, \mathrm{d}s - 0{\cdot}5h\Delta W_{l,i} = \frac{h^{3/2}}{\sqrt{12}} \zeta_{l,i}. \tag{25}$$

Finally, the desired double integral may be obtained as the sum of the following couple of zero-mean Gaussian random variables:

$$\begin{aligned} I_{l,0} &= (0{\cdot}5\Delta W_{l,i}) + \left\{ \int_{t_{i-1}}^{t_i} (W_l(s) - W_{l,i-1})\, \mathrm{d}s - 0{\cdot}5\Delta W_{l,i} \right\} \\ &= h^{3/2}\left( 0{\cdot}5\varsigma_{l,i} + \frac{1}{\sqrt{12}} \zeta_{l,i} \right). \end{aligned} \tag{26}$$

A specific advantage of the Newmark method is that the basic computational steps as described above basically remain the same irrespective of the dimensionality of the system. In case the system is non-linear, then for $\alpha, \beta \neq 1$ equations 21(a) and 21(b) constitute a set of coupled non-linear algebraic equations, which may be solved via a standard Newton–Raphson approach.

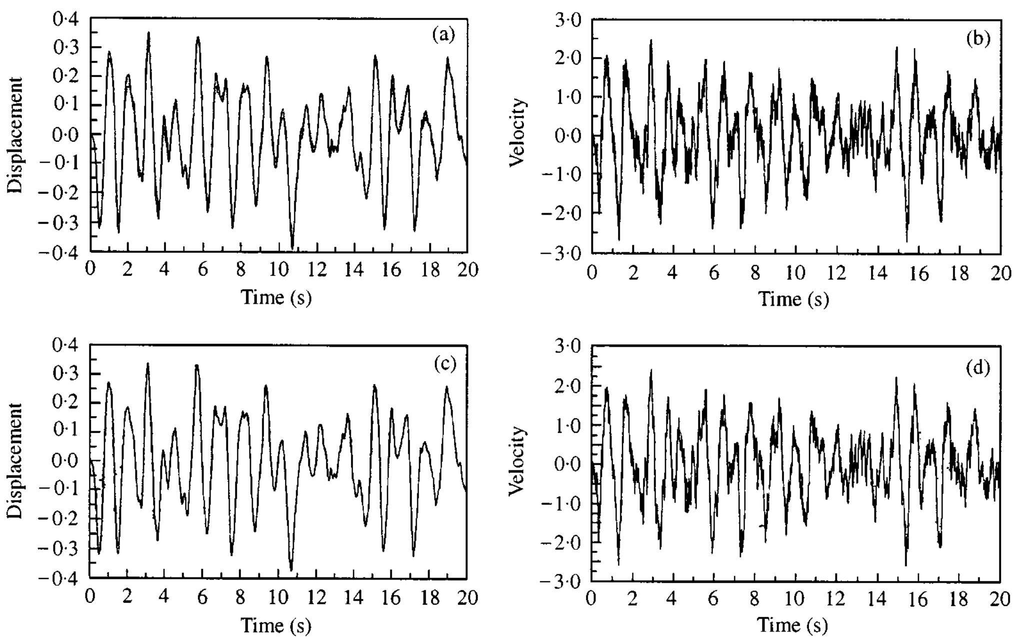


Figure 1. Displacement and velocity histories via SNM for different $\alpha, \beta$: $\varepsilon_1 = 0{\cdot}25$, $\varepsilon_2 = 1{\cdot}0$, $\varepsilon_3 = 0$, $\varepsilon_4 = 2{\cdot}0$, $\varepsilon_5 = 0{\cdot}0$. (a) Displacement histories for different values of $\alpha$ and $\beta$: ——, $\alpha = 0{\cdot}5$, $\beta = 0{\cdot}0$; ·········, $\alpha = 0{\cdot}5$, $\beta = 0{\cdot}25$; · · · ·, $\alpha = 0{\cdot}5$, $\beta = 0{\cdot}5$; ------, $\alpha = 0{\cdot}5$, $\beta = 0{\cdot}75$; - - - - -, $\alpha = 0{\cdot}5$, $\beta = 1{\cdot}0$. (b) Velocity histories for different values of $\alpha$ and $\beta$: ——, $\alpha = 0{\cdot}5$, $\beta = 0{\cdot}0$; ·········, $\alpha = 0{\cdot}5$, $\beta = 0{\cdot}25$; · · · ·, $\alpha = 0{\cdot}5$, $\beta = 0{\cdot}5$; ------, $\alpha = 0{\cdot}5$, $\beta = 0{\cdot}75$; - - - - -, $\alpha = 0{\cdot}5$, $\beta = 1{\cdot}0$. (c) Displacement histories for different values of $\alpha$ and $\beta$: ——, $\alpha = 0{\cdot}5$, $\beta = 0{\cdot}5$; ·········, $\alpha = 0{\cdot}25$, $\beta = 0{\cdot}5$; · · · ·, $\alpha = 0{\cdot}75$, $\beta = 0{\cdot}5$; ------, $\alpha = 1{\cdot}0$, $\beta = 0{\cdot}5$. (d) Velocity histories for different values of $\alpha$ and $\beta$: ——, $\alpha = 0{\cdot}0$, $\beta = 0{\cdot}5$; ·········, $\alpha = 0{\cdot}25$, $\beta = 0{\cdot}5$; · · · ·, $\alpha = 0{\cdot}75$, $\beta = 0{\cdot}5$; ------, $\alpha = 1{\cdot}0$, $\beta = 0{\cdot}5$.

In order to compare Newmark solutions in the stochastic regime with those obtained via an acceptable stochastic numerical scheme, the stochastic Heun scheme (SHS) is adopted. It is known that this scheme has local and global truncation errors of $O(h^{3/2})$ and $O(h)$, respectively [1], *provided that the system is driven by only one white-noise process*. In case of more than one independently evolving white-noise processes, local and global accuracy orders for SHS reduce to $O(h)$ and $O(h^{0\cdot 5})$ respectively (i.e., the same as Euler method). It is also to be noted here that there exist certain stochastic Runge–Kutta schemes [5] which lead to a higher local error order, provided that certain very stringent equalities involving the first and second derivatives of the drift and diffusion vectors are satisfied. Indeed, these equalities are not satisfied for the hardening Duffing system, thereby leaving the SHS method as the most accurate known integration tool. Thus, referring to the hardening Duffing SDE (20) with $W_1(t) = W_2(t) = W(t)$ (so that higher accuracy orders are maintained), one has the following map over the time interval $T_i = (t_{i-1}, t_i]$ to integrate the SDE based on SHS:

$$z_{1,i} = x_{1,i-1} + 0{\cdot}5(x_{2,i-1} + \tilde{z}_{2,n})h_i,$$

$$z_{2,i} = x_{2,i-1} + 0{\cdot}5(\psi(x_{1,i-1}, x_{2,i-1}, t_{i-1}) + \psi(\tilde{z}_{1,i}, \tilde{z}_{2,i}, t_i))h_i + [\varepsilon_4 + 0{\cdot}5\varepsilon_5(x_{1,i-1} + \tilde{z}_{1,i})\Delta W_i], \tag{27}$$

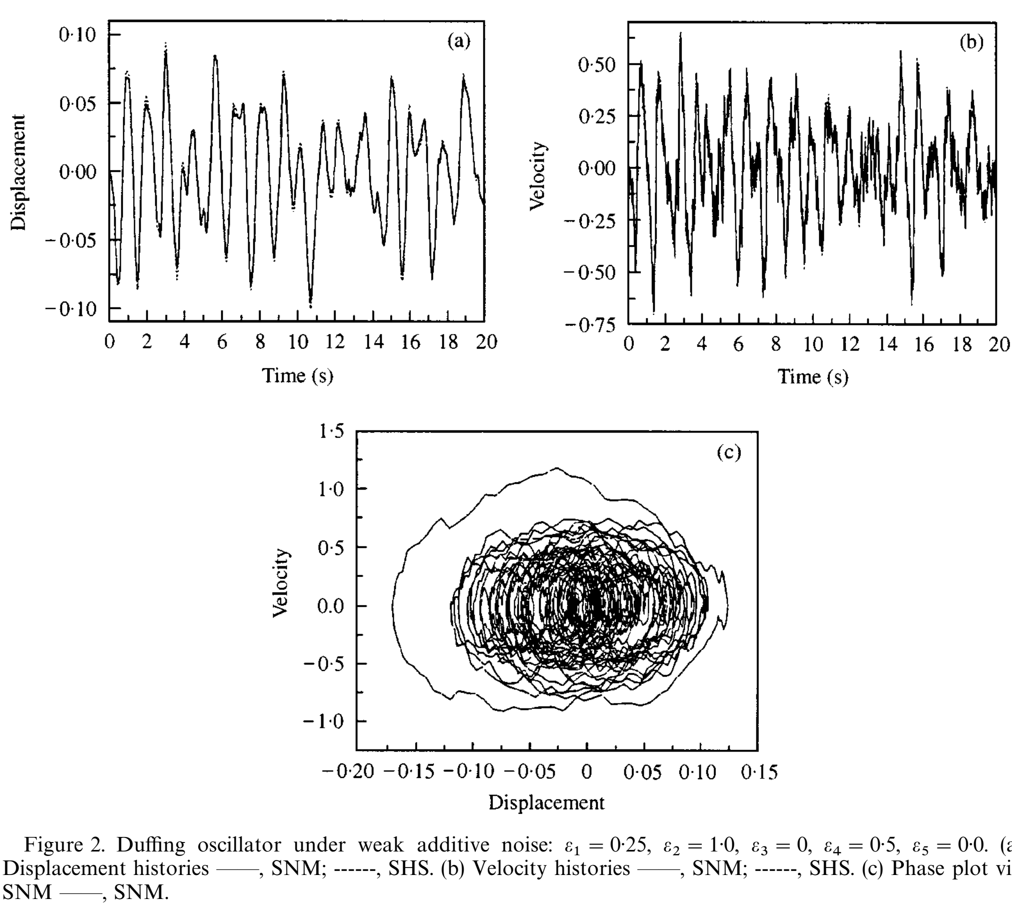


Figure 2. Duffing oscillator under weak additive noise: $\varepsilon_1 = 0{\cdot}25$, $\varepsilon_2 = 1{\cdot}0$, $\varepsilon_3 = 0$, $\varepsilon_4 = 0{\cdot}5$, $\varepsilon_5 = 0{\cdot}0$. (a) Displacement histories ——, SNM; ------, SHS. (b) Velocity histories ——, SNM; ------, SHS. (c) Phase plot via SNM ——, SNM.

where

$$h_i = t_i - t_{i-1},\ \tilde{z}_{1,i} = x_{1,i-1} + x_{2,i-1}, h_i,$$

$$\tilde{z}_{2,i} = x_{2,i-1} + \psi(x_{1,i-1}, x_{2,i-1}, t_{i-1})h_i + (\varepsilon_4 + \varepsilon_5 x_{1,i-1}\Delta W_i),$$

$$\psi(x_1, x_2, t) = -2\pi\varepsilon_1 x_2 - 4\pi^2\varepsilon_2(1 + x_1^2)x_1 + 4\pi^2\varepsilon_3\cos(2\pi t).$$

In equation (27), $(z_{1,i}, z_{2,i})$ is the SHS approximation vector to $(x_{1,i}, x_{2,i})$ and $(x_{1,i-1}, x_{2,i-1})$ constitute the known initial condition vector. In order to compare the results of SNM with that of SHS, it is required that the same realizations of standard Wiener increments, $\Delta W_i$ be used. It needs to be stressed that in case of multiple white-noise excitations (i.e., $W_1(t)$ and $W_2(t)$ are distinct and independently evolving), *there are no restrictions on the applicability of the Newmark procedure*, even though SHS is generally not applicable for such cases.

A consistent time step size $h = 0{\cdot}01$ has been adopted in all the following numerical results. To understand the effect of arbitrary solution parameters, $\alpha$ and $\beta$, on SNM, displacement and velocity histories under combined additive and multiplicative stochastic excitations are plotted in Figure 1(a–d) for different choices of these parameters in [0, 1]. It can be seen that the trajectories do not sensitively depend on the choice of $\alpha$ and $\beta$. While choosing $\alpha = \beta = 1$ makes the Newmark map explicit (and hence computationally faster),

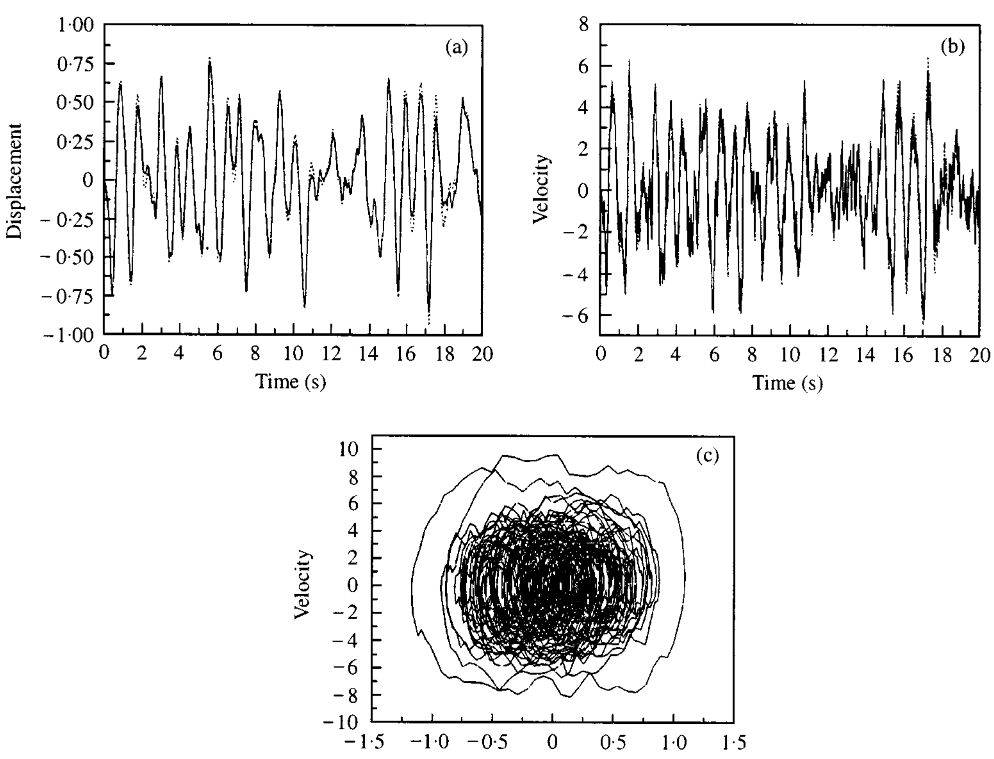


Figure 3. Duffing oscillator under medium additive noise. $\varepsilon_1 = 0{\cdot}25$, $\varepsilon_2 = 1{\cdot}0$, $\varepsilon_3 = 0$, $\varepsilon_4 = 5{\cdot}0$, $\varepsilon_5 = 0{\cdot}0$. (a) Displacement histories ——, SNM; ------, SHS. (b) Velocity histories ——, SNM; ------, SHS. (c) Phase plot via SNM. ——, SNM.

an implicit scheme is known to have far better stability characteristics, especially for larger time step sizes, and hence $\alpha = \beta = 0{\cdot}5$ has been consistently chosen in all the numerical results to follow. In Figures 2–4, displacement and velocity histories along with phase plots of SNM-based solutions of the oscillator under weak, medium and strong intensities of additive white-noise inputs are shown. No deterministic and multiplicative stochastic inputs are assumed to be acting on the oscillator in these examples. Comparisons of time histories obtained via SNM with those via SHS appear to be quite close. Figure 5(a–d) show displacement and velocity histories, again obtained via both SNM and SHS, under combined additive and multiplicative excitations with the deterministic forcing amplitude parameter $\varepsilon_3 = 0$. The two methods are again found to be in good agreement even for a high multiplicative noise intensity, $\varepsilon_5 = 10$. When the hardening oscillator is driven only by a deterministic sinusoidal input, so that the amplitude parameter $\varepsilon_3$ is reasonably small, the response is in the form of a one-periodic (elliptic or dumb-bell shaped) orbit. Figures 6 and 7 show the effects of low and strong additive noise intensities on one such one-periodic orbit ($\varepsilon_3 = 0{\cdot}2$). While a weak additive noise only makes orbit noisy, a strong noise intensity completely smears out the periodic structure, as seen in the phase plot of Figure 7(c). So far, time history comparisons between SHS and SNM are consistently found to yield satisfactory results. On the other hand, for locally unstable orbits, such as those encountered during chaos or quasi-periodicity, SNM may err unacceptably in computing the velocity components. One such chaotic attractor under a weak additive stochastic excitation ($\varepsilon_4 = 0{\cdot}5$) is plotted in Figure 8(a) and 8(b) using SNM and SHS respectively. In

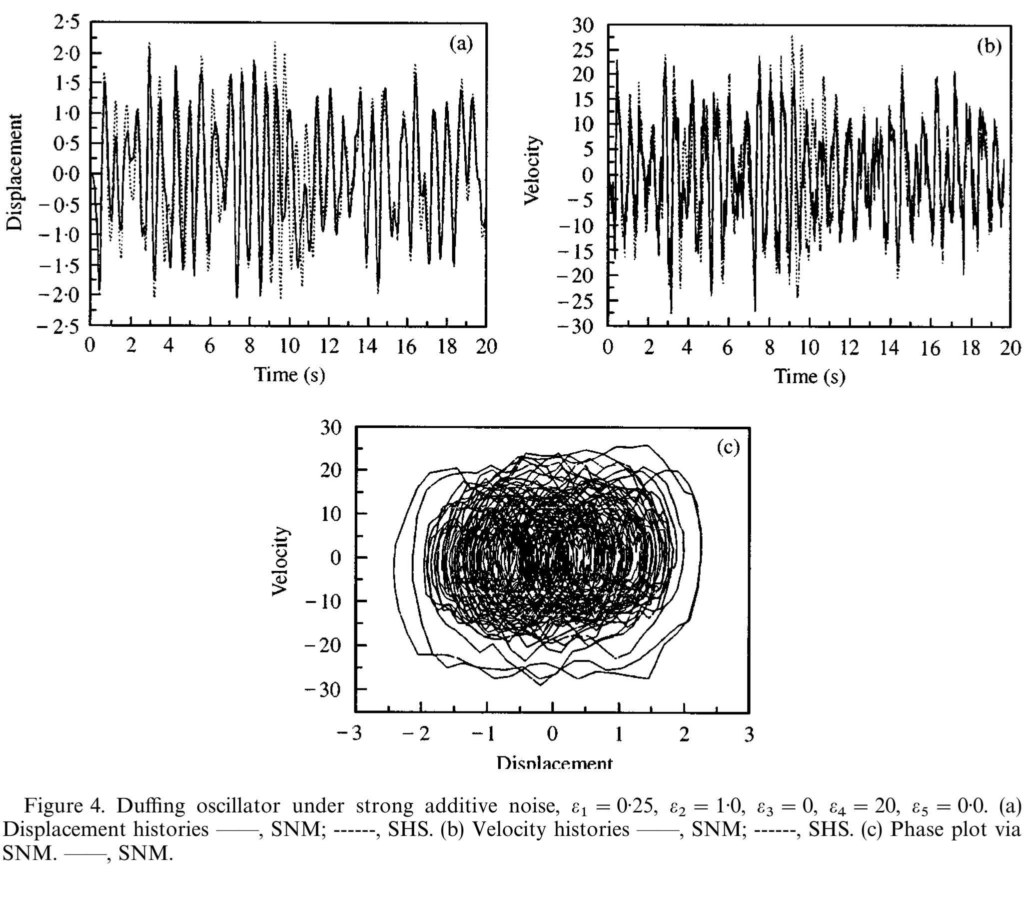


Figure 4. Duffing oscillator under strong additive noise, $\varepsilon_1 = 0{\cdot}25$, $\varepsilon_2 = 1{\cdot}0$, $\varepsilon_3 = 0$, $\varepsilon_4 = 20$, $\varepsilon_5 = 0{\cdot}0$. (a) Displacement histories ——, SNM; ------, SHS. (b) Velocity histories ——, SNM; ------, SHS. (c) Phase plot via SNM. ——, SNM.

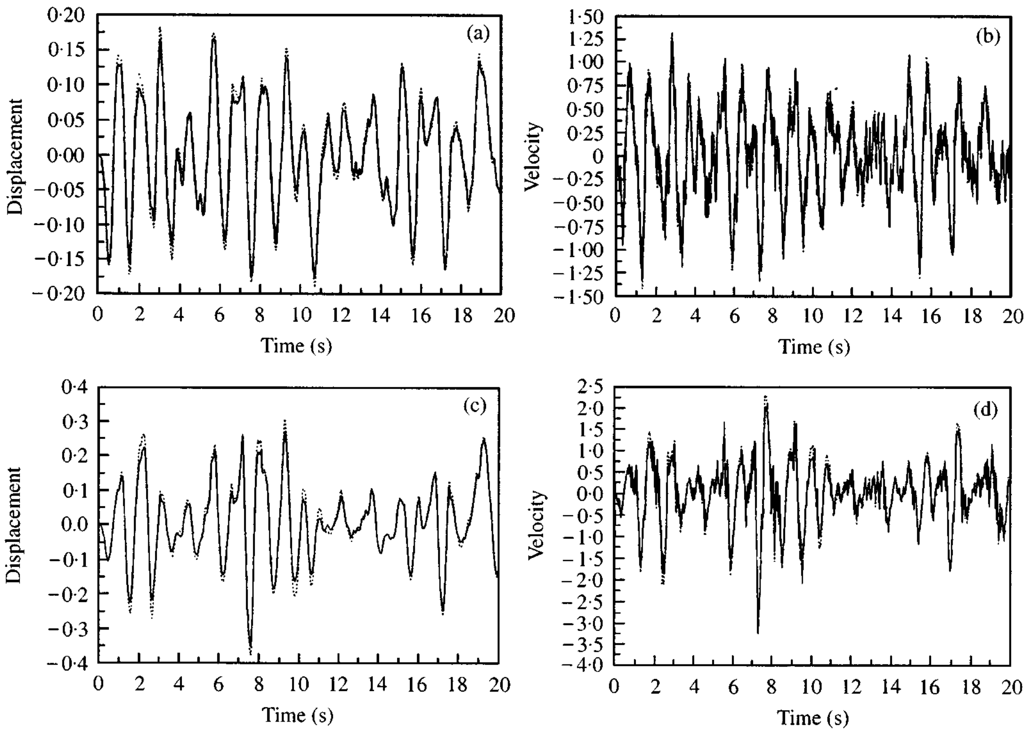


Figure 5. Duffing oscillator under combined additive and multiplicative noises, $\varepsilon_1 = 0{\cdot}25$, $\varepsilon_2 = 1{\cdot}0$, $\varepsilon_3 = 0$, $\varepsilon_4 = 0{\cdot}5$. (a) Displacement histories, $\varepsilon_5 = 1{\cdot}0$, ——, SNM; ------, SHS. (b) Velocity histories, $\varepsilon_5 = 1{\cdot}0$, ——, SNM; ------, SHS. (c) Displacement histories, $\varepsilon_5 = 10{\cdot}0$, ——, SNM; ------, SHS. (d) Velocity histories, $\varepsilon_5 = 10{\cdot}0$, ——, SNM; ------, SHS.

Figure 8(c) and 8(d), phase plots of the strange attractor, respectively, obtained via SNM and SHS, under a stronger additive noise intensity ($\varepsilon_4 = 20$) are shown. Since the global error in velocity computation is $O(h^{1/2})$ in SNM as against $O(h)$ in SHS, the phase plots obtained for this kind of an orbit via SNM are a little distorted along the velocity axis. One must therefore exercise caution while assessing the non-linear response during locally unstable regimes using SNM. In all the cases, however, one achieves a lower global displacement error of $O(h^{3/2})$ via SNM than a global error order of $O(h)$ in SHS. Next, effects of weak and strong multiplicative noise intensities on a typical one-periodic attractor (with the deterministic forcing amplitude parameter $\varepsilon_3 = 0{\cdot}2$ as in Figures 6 and 7) are shown in Figures 9 and 10. For a weak multiplicative intensity level, time history comparisons between SNM and SHS are quite good (Figure 9(a) and (b)) and, as seen from the phase plot of Figure 9(c), the periodic orbit becomes noisy. Closeness of SNM and SHS-based time-history comparisons for a stronger multiplicative intensity level, however, becomes less prominent (Figure 10(a) and 10(b)). Nevertheless, the phase plots, generated by these two methods and plotted in Figure 10(c) and 10(d), remain qualitatively the same even in this case.

An important and desirable property of any stochastic numerical method is its numerical stability [6]. Let $\bar{x}^\delta(t, \bar{x}_0^\delta, \omega)$ and $\hat{x}^\delta(t, \hat{x}_0^\delta, \omega)$ with $\delta \in (0, \Delta_0]$ denote two separable SNM-based solutions based on the initial conditions $\bar{x}_0^\delta$ and $\hat{x}_0^\delta$, respectively, and for a fixed $\omega \in \Omega$. Then the SNM-solution $\bar{x}^\delta(t, \bar{x}_0^\delta, .)$ is termed as stochastically numerically stable if there exists a positive constant $\Delta_0$ such that the following limiting condition is satisfied for

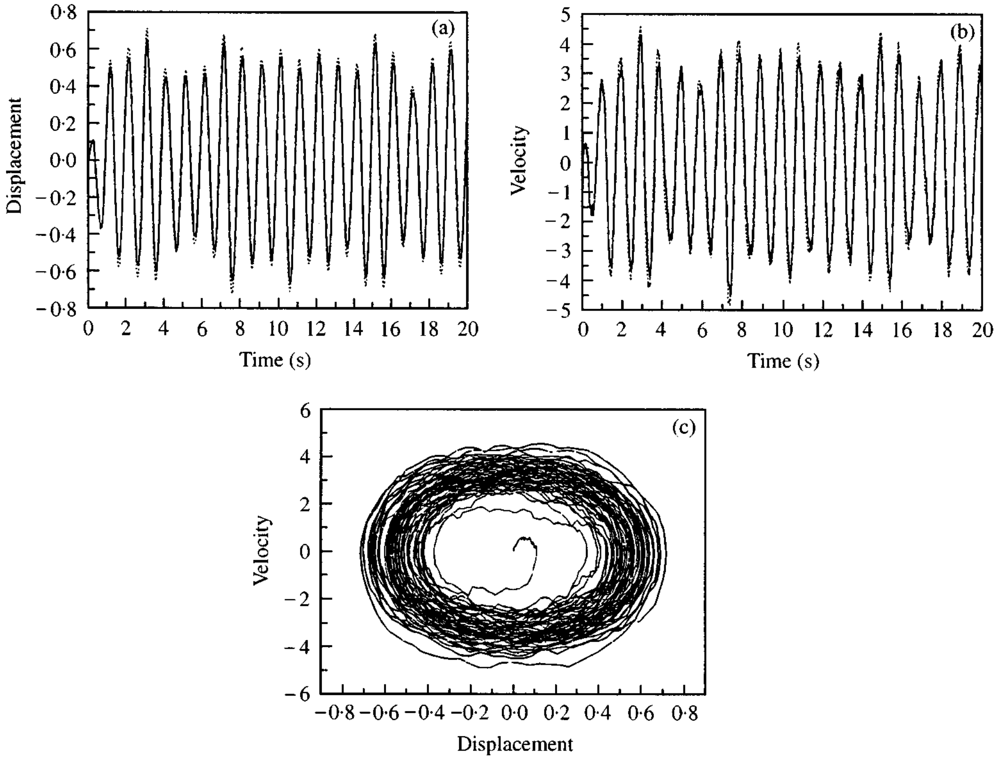


Figure 6. Duffing oscillator under combined deterministic excitation and weak additive noise, $\varepsilon_1 = 0{\cdot}25$, $\varepsilon_2 = 1{\cdot}0$, $\varepsilon_3 = 0{\cdot}2$, $\varepsilon_4 = 1{\cdot}0$, $\varepsilon_5 = 0{\cdot}0$. (a) Displacement histories ——, SNM; ------, SHS. (b) Velocity histories ——, SNM; ------, SHS. (c) Phase plot via SNM. ——, SNM.

each $\delta \in (0, \Delta_0)$ and for each $\varepsilon > 0$:

$$\lim_{|\bar{x}^\delta(t) - \hat{x}^\delta(t)| \to 0} \; \sup_{t_0 < t \leqslant T} P(|\bar{x}^\delta(t) - \hat{x}^\delta(t)| \geqslant \varepsilon) = 0, \tag{28}$$

where $T$ denotes the right boundary of a finite time interval. Obviously, the stochastic numerical stability for the SNM algorithm is best tested against an undamped response (which has a zero divergence in the phase space). Thus, SNM-based solutions $\tilde{x}(t)$ and $\dot{\tilde{x}}(t)$ for two such trajectories of the undamped Duffing equation (20) (i.e., with $\varepsilon_1 = 0$) emerging from two closely separated initial conditions are shown in Figure 11(a) and 11(b) for the same realization of the Wiener process (implying, thereby, that $\omega$ is fixed). The fact that the two SNM-based trajectories remain close to each other (at least for over a considerable initial interval) serves as a pointer towards the stochastic numerical stability of the proposed scheme.

Since the only additional numerical task for implementing SNM over its deterministic counterpart is only to generate a few random numbers (which are used to exactly evaluate a few stochastic integrals), the speed of stochastic integration should be comparable with the deterministic case. Moreover, even for a very large linear stochastic system, one has to solve a system of linear algebraic equations $[A]\{\tilde{X}_i\} = \{b(\tilde{X}_{i-1}, t_{i-1})\}$ via SNM, where the bandwidth (or front-width) structure of $[A]$ is no different from the original system matrices $[M]$, $[C]$ and $[K]$.

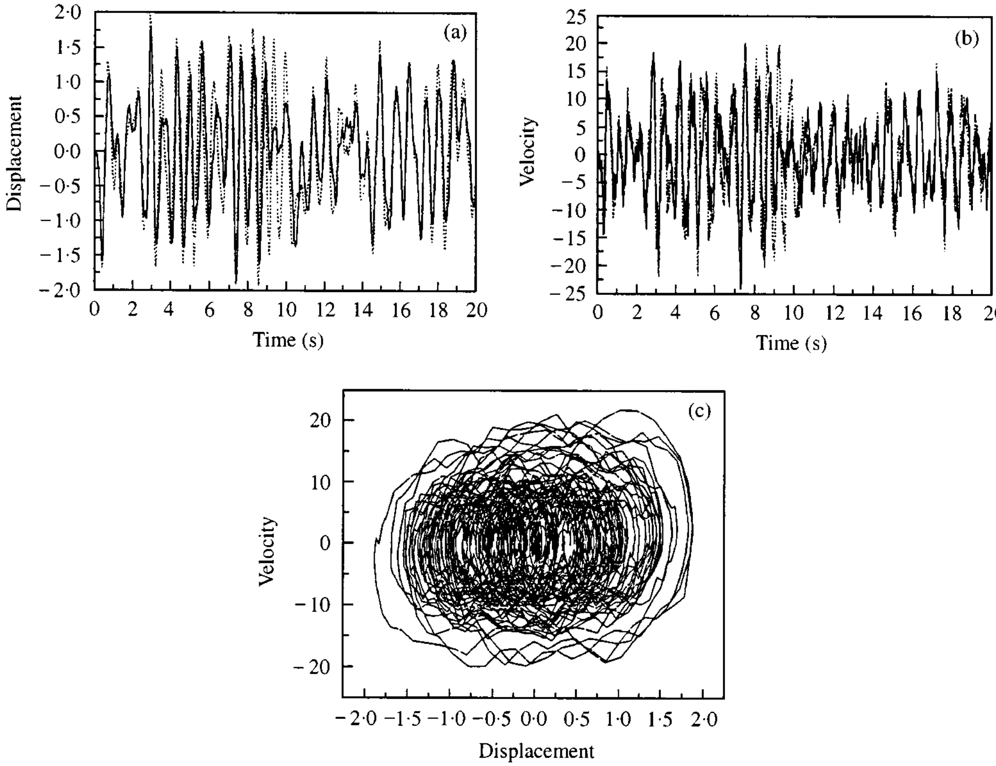


Figure 7. Duffing oscillator under combined deterministic excitation and strong additive noise, $\varepsilon_1 = 0{\cdot}25$, $\varepsilon_2 = 1{\cdot}0$, $\varepsilon_3 = 0{\cdot}2$, $\varepsilon_4 = 15{\cdot}0$, $\varepsilon_5 = 0{\cdot}0$. (a) Displacement histories ——, SNM; ------, SHS. (b) Velocity histories ——, SNM; ------, SHS. (c) Phase plot via SNM. ——, SNM.

## 5. DISCUSSION AND CONCLUSIONS

A stochastic Newmark method (SNM) for direct time integration of engineering dynamical systems driven by additive or multiplicative (filtered) white-noise excitations is proposed. The basis of this new development is a two-parameter implicit stochastic Taylor expansion of both displacement and velocity components. These Taylor expansions may be based either on Ito or Stratonovich calculus. Some of the higher order terms involving multiple integrals of the associated Wiener processes, have been left out of these expansions, thereby rendering the present approach computationally fast and easy to implement. Rigorous error estimates, including a discussion on the consequences of retaining or leaving out some of these terms, have been provided. A limited numerical study on the application of the method for pathwise integration of a non-linear hardening Duffing oscillator under additive and multiplicative white-noise excitations is undertaken. These results have been compared with those obtained via the stochastic Heun scheme. For most of the response regimes, the reported results are indicative of the consistency, accuracy and stochastic numerical stability of the proposed scheme.

Since the Newmark method, as applied to a linear dynamical system, leads to a linear map, the same can be used to obtain a closed-form map for the moment functions. For non-linear problems, Newmark's implicit stochastic map may also be utilized to approximately obtain the associated probability density functions. Finally one may derive,

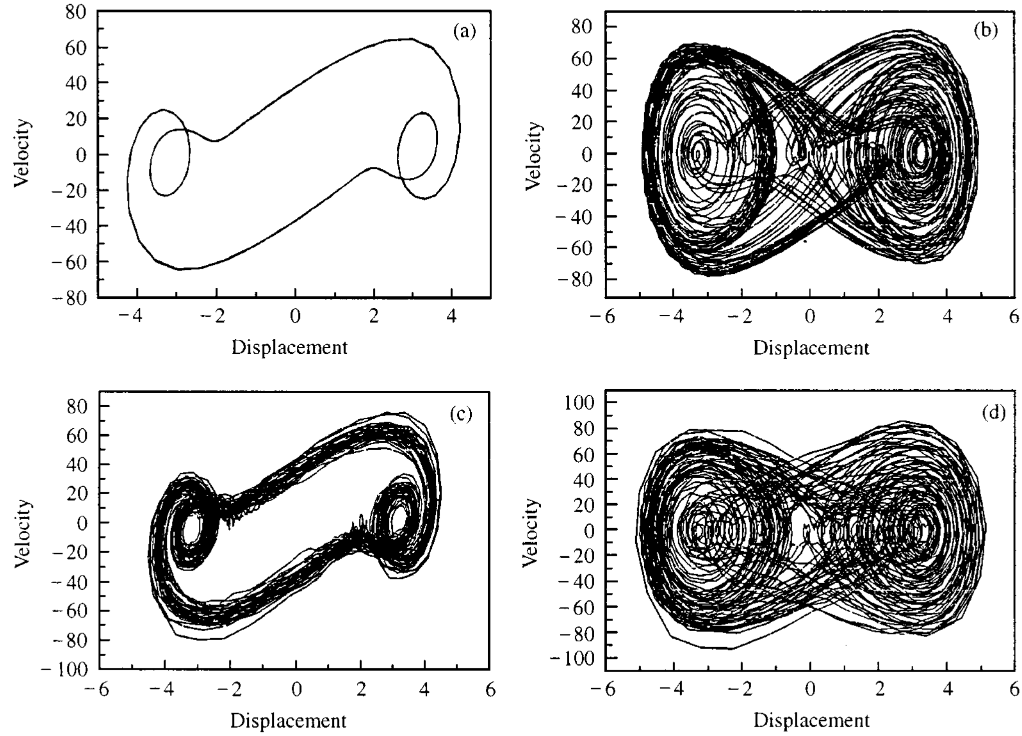


Figure 8. A chaotic attractor under additive noise, $\varepsilon_1 = 0{\cdot}25$, $\varepsilon_2 = 1{\cdot}0$, $\varepsilon_3 = 41$, $\varepsilon_5 = 0{\cdot}0$. (a) Phase plot via SNM, $\varepsilon_4 = 0{\cdot}5$ ——, SNM. (b) Phase plot via SHS, $\varepsilon_4 = 0{\cdot}5$ ——, SHS. (c) Phase plot via SNM, $\varepsilon_4 = 20{\cdot}0$ ——, SNM. (d) Phase plot via SHS, $\varepsilon_4 = 20{\cdot}0$ ——, SHS.

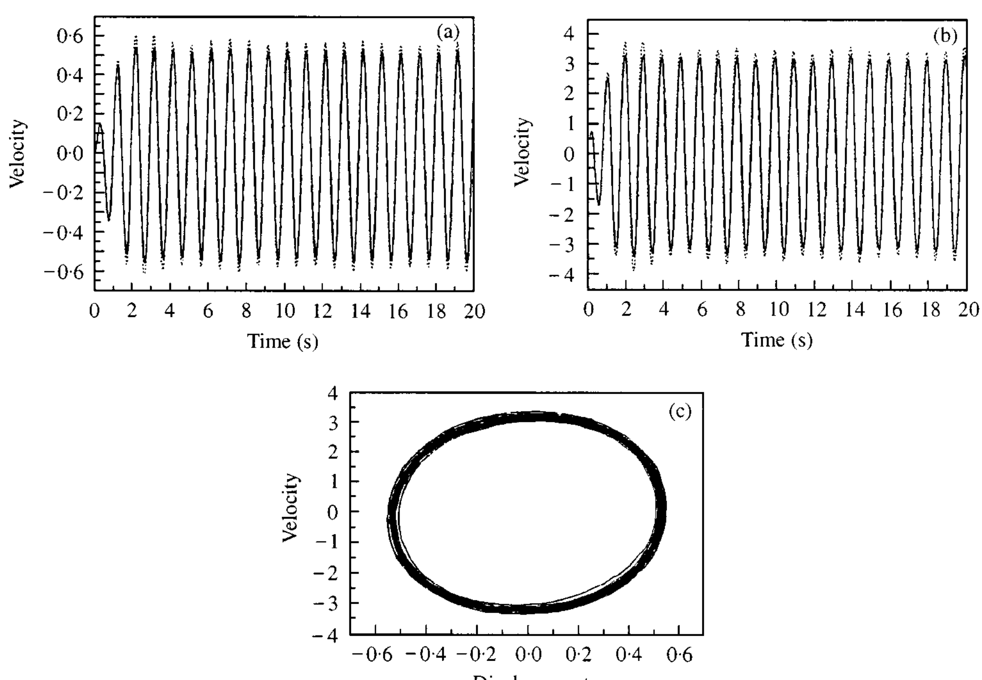


Figure 9. Duffing oscillator under deterministic excitation and weak multiplicative noise, $\varepsilon_1 = 0{\cdot}25$, $\varepsilon_2 = 1{\cdot}0$, $\varepsilon_3 = 0{\cdot}2$, $\varepsilon_4 = 0{\cdot}0$, $\varepsilon_5 = 0{\cdot}5$. (a) Displacement histories ——, SNM; ------, SHS. (b) Velocity histories ——, SNM; ------, SHS. (c) Phase plot via SNM. ——, SNM.

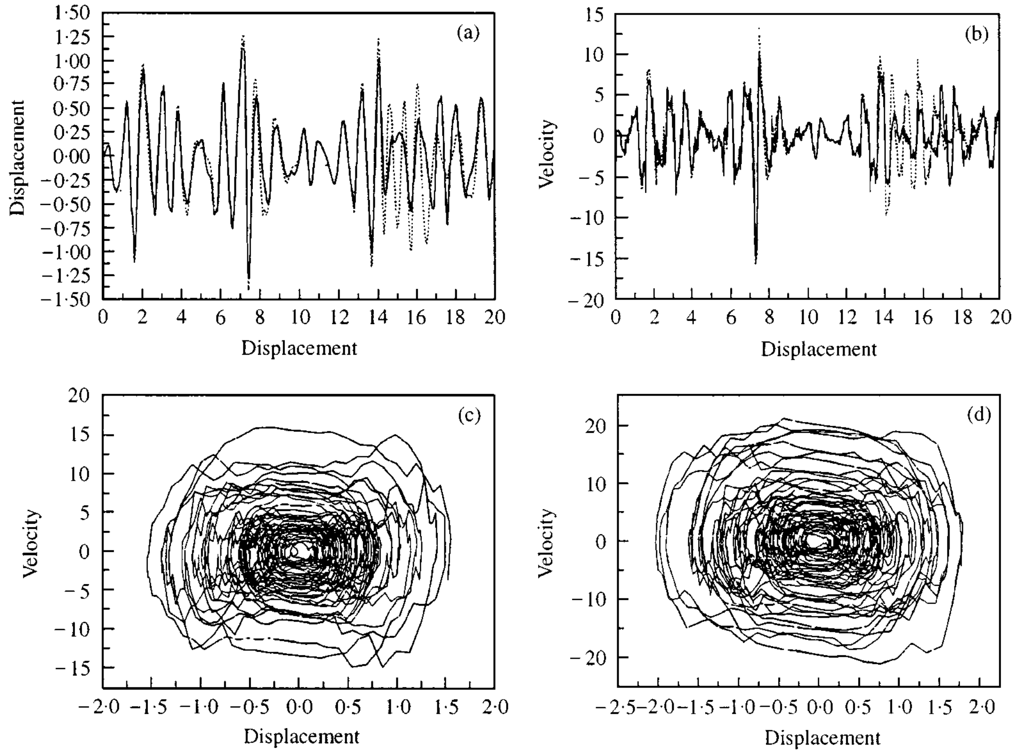


Figure 10. Duffing oscillator under deterministic excitation and strong multiplicative noise, $\varepsilon_1 = 0{\cdot}25$, $\varepsilon_2 = 1{\cdot}0$, $\varepsilon_3 = 0{\cdot}2$, $\varepsilon_4 = 0{\cdot}0$, $\varepsilon_5 = 15$. (a) Displacement histories ——, SNM; ------, SHS. (b) Velocity histories ——, SNM; ------, SHS. (c) Phase plot via SNM ——, SNM. (d) Phase plot via SHS. ——, SHS.

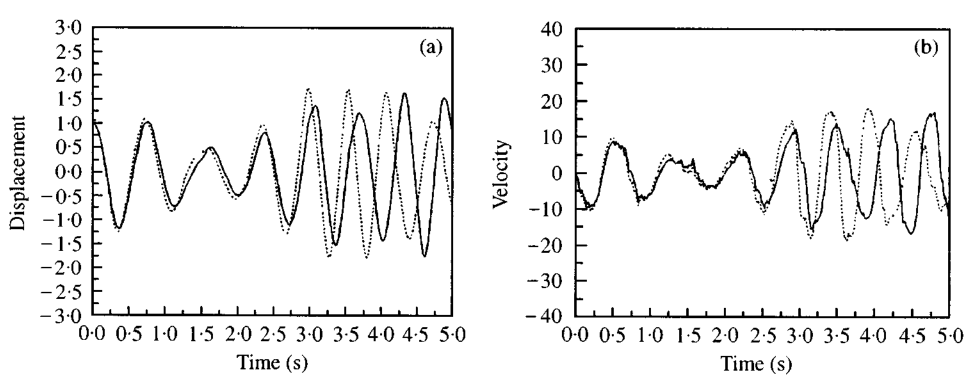


Figure 11. Stochastic numerical stability of SNM as applied to undamped Duffing oscillator, $\varepsilon_1 = 0{\cdot}0$, $\varepsilon_2 = 1{\cdot}0$, $\varepsilon_3 = 0{\cdot}2$, $\varepsilon_4 = 5{\cdot}0$, $\varepsilon_5 = 5{\cdot}0$: (a) Displacement histories via SNM ——, Ini. Displ. = 1·0, Ini. Vel. = 0·0; ------, Ini. Displ. = 1·1, Ini. Vel. = 0·0. (b) Velocity histories via SNM ——, Ini. Displ. = 1·0, Ini. Vel. = 0·0; ------, Ini. Displ. = 1·1, Ini. Vel. = 0·0.

at the expense of a substantially higher computational overhead, higher order stochastic Newmark algorithms by incorporating higher order multiple integrals into the stochastic Taylor expansions. The method, as presented in this paper, is simple and readily implementable to handle large m.d.o.f. systems of engineering interest.

## REFERENCES


1. N. M. Newmark 1959 *Journal of Engineering Mechanics* (*American Society of Civil Engineers*) **85**, 67–94. A method for computation of structural dynamics.
2. I. Miranda, R. M. Ferencz and T. J. R. Hughes 1989 *International Journal of Earthquake Engineering and Structural Dynamics* **18**, 643–655. An improved implicit-explicit time integration method for structural dynamics.
3. T. Belytschko and T. J. R. Hughes, Editors 1983 *Computational Methods for Transient Analysis*. Dordrecht: North Holland.
4. O. C. Zienkiewicz and R. L. Taylor 1991 *The Finite Element Method*, Vol. 2. U.K.: McGraw-Hill.
5. T. C. Gard 1988 *Introduction to Stochastic Differential Equations*. New York: Marcel Dekker Inc.
6. P. E. Kloeden and E. Platen 1999 *Numerical Solution of Stochastic Differential Equations*. Berlin: Springer.
7. G. Maruyama Rend *Circuit Material*, *Palermo* **4**, 48–90. Continuous Markov processes and stochastic equations.
8. I. I. Gikhman and A. V. Skorokhod 1972 *Stochastic Differential Equations*. Berlin: Springer.
9. S. Kanagawa 1997 *Nonlinear Analysis* **30**, 4101–4104. Confidence intervals of discretized Euler–Maruyama approximate solutions of SDEs.
10. G. N. Milstein 1974 *Theory of Probability and Application* **19**, 557–562. Approximate integrations of stochastic differential equations.
11. W. Wagner and E. Platen 1978 *Preprint*, ZIMM. Berlin: Akad. Wissenschaften, DDR. Approximation of Ito integral equations.
12. G. N. Milstein 1995 *Numerical Integration of Stochastic Differential Equations*. Dordrecht: Kluwer Academic Publishers.
13. P. E. Kloeden and E. Platen 1992 *Journal of Statistical Physics* **66**, 283–314. Higher order implicit strong numerical schemes for stochastic differential equations.
14. W. Rumelin 1982 *SIAM Journal of Numerical Analysis* **19**, 604–613. Numerical treatment of stochastic differential equations.
15. C. W. S. To 1986 *Computers and Structures* **23**, 813–818. The stochastic central difference method in structural dynamics.
16. C. W. S. To 1988 *Computers and Structures* **30**, 865–874. Direct integration operations and their stability for random response of multi-degree-of-freedom systems.
17. C. W. S. To 1988 *Computers and Structures* **29**, 451–457. Recursive expressions for random response of non-linear systems.
18. C. W. S. To 1992 *Computers and Structures* **44**, 667–673. A stochastic version of Newmark family of algorithms for discretized dynamical systems.
19. S. W. Zhang and H. H. Zhao 1992 *Journal of Sound and Vibration* **159**, 182–188. Effects of time step in stochastic central difference method.
20. L. Zhang, J. W. Zu and Z. Zheng 1999 *Computers and Structures* **70**, 557–568. The stochastic Newmark algorithm for random analysis of multi-degree-of-freedom nonlinear systems.
21. B. Miao 1993 *Computers and Structures* **46**, 979–983. Direct integration variance prediction of random response of nonlinear systems.
22. D. Roy 2000 *International Journal of Nonlinear Dynamics* **23**, 225–258. Explorations of the phase space linearization method for deterministic and stochastic non-linear dynamical systems.